

# Seismic Behavior of Structures with Building Mass Damper Design

**Kuo-Chun Chang**

*Professor, Department of Civil Engineering, National Taiwan University, Taipei, Taiwan*

**Jenn-Shin Hwang**

*Professor, Department of Construction Engineering, Taiwan University of Science and Technology, Taipei, Taiwan*

**Shiang-Jung Wang**

*Associate Researcher, National Center for Research on Earthquake Engineering, Taipei, Taiwan*

**Bo-Han Lee**

*Ph. D. Candidate; National Taiwan University, Taiwan*

**Ying-Hsuan Chen**

*Graduate Student; National Taiwan University, Taiwan*



## SUMMARY:

In this paper, the feasibility of the incorporation of the tuned mass damper (TMD) design concept into a mid-story isolated building, namely building mass damper (BMD) design thereafter, is analytically and experimentally studied. The stiffness and damping of the BMD system can be provided by the mid-story isolation system composed of seismic isolation bearings and additional viscous dampers. Most importantly, the superstructure can serve as a tuned absorber mass such that the size limitation of the conventional TMD design method can be overcome. A simplified three-lumped-mass structural model, in which three lumped masses are assigned at the superstructure, isolation layer and substructure, is used to represent the dynamic characteristics of a building with BMD design. The objective function to determine the optimum BMD design parameters is that, the damping ratios of three translation modes of the simplified structural model are essential and should be very close. Based on the sensitive analysis results, it is indicated that the BMD design concept is really doable with an acceptable damping ratio demand. Several scaled down structural models with different BMD design parameters are also numerically and experimentally studied. It is revealed that the optimum BMD design method, which possesses two predominant modes, is really effective for the seismic protection of both the superstructure (tuned mass structure) and substructure (main structure).

*Keywords: Isolation, damper, mid-story*

## 1. INTRODUCTION

The TMD system is an energy absorbing device essentially consisting of a mass, spring and damper to reduce the undesirable vibrations of the attached vibrating system subjected to harmonic excitations. This technology has already been applied in many high-rise buildings to mitigate the wind-induced vibrations. The optimum design parameters for a building structure with the TMD system can be determined using different objective functions. Because of a significant phase lag between the main structure and TMD system, the dynamic responses of the main structure induced by wind or seismic excitations can be mitigated effectively.

For particular concerns of architectural functionality and construction feasibility, the mid-story isolation design method in which the isolation system is incorporated into the mid-story rather than the base of a building is recently gaining popularity for seismic protection of building structures. The effectiveness of mid-story isolation design in reducing seismic demand on the superstructure above the isolation system has been numerically and experimentally proved in many previous researches. It was also indicated that the improper design for the substructure below the isolation system may result in adverse effects on the seismic performance of the isolated superstructure, e.g. the enlarged acceleration

responses at the superstructure or coupling of higher modes.

In order to combine the advantages of conventional TMD and mid-story isolation design for seismic protection of both the superstructure (or tuned absorber mass) and substructure (or main structure) of a building structure, a new structural design concept, denoted as building mass damper (BMD) design, is proposed in this study. In a building structure using BMD design, the superstructure serves as a tuned absorber mass whose stiffness and damping can be provided by the isolation system composed of elastomeric bearings and additional dampers. In that case, the size limitation for the tuned absorber mass of conventional TMD design can be easily overcome. A simplified three-lumped-mass structural model is rationally assumed to represent a building structure with the BMD system considering the dynamic characteristics of the superstructure and substructure. The motion equation of the simplified structural model is formulated in terms of the author-defined mass ratios, frequency ratios and damping ratios. The objective function to determine the optimum design parameters for the BMD system is that three modal damping ratios which are dominant respectively for the superstructure, isolated layer and substructure in the direction of interest are important and should be taken as an approximately equal value. Accordingly, the interaction among the superstructure, isolated layer and substructure of a building structure using BMD design can be taken into account in the simplified structural model. The thorough sensitive analysis is performed to discuss the feasibility of the proposed BMD design method. In addition, a shaking table test scheme is conducted to verify the effectiveness of the BMD system on the seismic protection of a building structure.

## 2. ANALYTICAL STUDY

### 2.1. Three-Lumped-Mass Structural Model

In a building structure with the BMD system, the superstructure (or tuned absorber mass) may be a multi-story structure and is generally much weightier than a conventional tuned absorber mass. Therefore, three lumped masses are suggested to be respectively assigned at the substructure, isolation layer and superstructure. This simplified structural mode is denoted as three-lumped-mass structural model thereafter and is shown in Fig. 2.1. The motion equation of the simplified structural model can be written as

$$M \ddot{u} + C \dot{u} + K u = -M \ddot{u}_g \quad (2.1)$$

$$M = \begin{bmatrix} m_1 & 0 & 0 \\ 0 & m_2 & 0 \\ 0 & 0 & m_3 \end{bmatrix} \quad (2.2)$$

$$C = \begin{bmatrix} c_1 + c_2 & -c_2 & 0 \\ -c_2 & c_2 + c_3 & -c_3 \\ 0 & -c_3 & c_3 \end{bmatrix} \quad (2.3)$$

$$K = \begin{bmatrix} k_1 + k_2 & -k_2 & 0 \\ -k_2 & k_2 + k_3 & -k_3 \\ 0 & -k_3 & k_3 \end{bmatrix} \quad (2.4)$$

where  $u_1$ ,  $u_2$  and  $u_3$  = the lateral displacements of the substructure, isolation layer and superstructure relative to ground, respectively;  $\ddot{u}_g$  = the ground acceleration;  $m_1$ ,  $m_2$  and  $m_3$  = the generalized seismic reactive masses of the substructure, isolation layer and superstructure, respectively;  $k_1$  and  $k_3$  = correspondingly the generalized elastic lateral stiffnesses of the substructure and superstructure;  $k_2$  = the effective lateral stiffness of the isolation system;  $c_1$  and  $c_3$  = respectively the viscous damping coefficients of the substructure and superstructure; and  $c_2$  = the equivalent viscous damping coefficient of the isolation system. The motion equation can also be characterized using the author-defined mass ratios, frequency ratios and damping ratios. The mass ratio  $\mu_i$  is defined as each lumped mass  $m_i$  divided by the substructure mass  $m_1$

$$\mu_i = \frac{m_i}{m_1}, i=2, 3 \quad (2.5)$$

where  $i=2$  and  $3$  represent the isolation layer and superstructure, respectively. The frequency ratios  $f_2$  and  $f_3$  are defined as

$$f_i = \frac{\omega_i}{\omega_1}, i=2, 3 \quad (2.6)$$

where  $\omega_1 = \sqrt{k_1/(m_1 + m_2 + m_3)}$ ,  $\omega_2 = \sqrt{k_2/(m_2 + m_3)}$  and  $\omega_3 = \sqrt{k_3/m_3}$  are defined to be the nominal frequencies of the substructure, isolation layer and superstructure, respectively. The component damping ratios of the substructure, isolation layer and superstructure can be given by

$$\xi_1 = \frac{c_1}{2(m_1 + m_2 + m_3)\omega_1} \quad (2.7)$$

$$\xi_2 = \frac{c_2}{2(m_2 + m_3)\omega_2} \quad (2.8)$$

$$\xi_3 = \frac{c_3}{2m_3\omega_3} \quad (2.9)$$

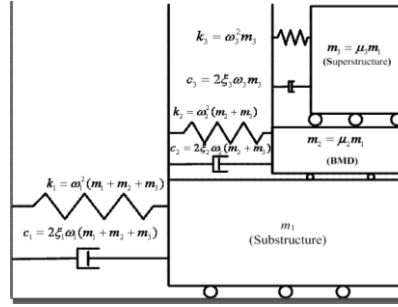


Figure 2.1 Simplified three-lumped-mass structural model

## 2.2 Optimum Design Criterion for Structure with BMD System

The system matrix  $A'$  of Equation (2.1), as given in Equation (2.10), can be obtained in terms of the nominal frequency  $\omega_1$ , mass ratios  $\mu_2$  and  $\mu_3$ , frequency ratios  $f_2$  and  $f_3$ , and component damping ratios  $\xi_1$  and  $\xi_2$ .

$$A' = \begin{bmatrix} 0_{3 \times 3} & I_{3 \times 3} \\ -M_{3 \times 3}^{-1} K_{3 \times 3} & -M_{3 \times 3}^{-1} C_{3 \times 3} \end{bmatrix} \quad (2.10)$$

The complex eigenvalues of Equation (2.10) in the direction of interest can be determined in the form of conjugate pairs

$$\lambda'_{r,r+1} = -\omega'_r \xi'_r \pm i \omega'_r \sqrt{1 - \xi'^2_r} \quad (2.11)$$

where  $\lambda'_r$  is the  $r^{th}$  modal eigenvalue of the system;  $\lambda'_{r+1}$  is the conjugate of  $\lambda'_r$ ;  $\omega'_r$  and  $\xi'_r$  are the  $r^{th}$  modal natural frequency and the  $r^{th}$  modal damping ratio of the system, respectively; and  $i$  is the unit imaginary number (i.e.  $i = \sqrt{-1}$ ). The objective function to determine the optimum design parameters for the BMD system is that three modal damping ratios which are dominant respectively

for the response mitigation of the superstructure, isolated layer and substructure are important and should be taken as an approximately equal value, i.e.  $\xi_1 \cong \xi_3 \cong \xi_5$ .

### 2.3 Sensitivity Analysis

After the reasonable values of  $\mu_2$ ,  $\mu_3$ ,  $\xi_1$  and  $\xi_3$  are determined, the optimum design parameters  $\xi_2$ ,  $f_2$  and  $f_3$  can be calculated in accordance with the aforementioned objective function. The optimum design parameters  $\xi_2$ ,  $f_2$  and  $f_3$  varying with respect to  $\mu_2$  and  $\mu_3$  considering different damping ratios of the substructure and superstructure are illustrated in Figs. 2.2, 2.3 and 2.4, respectively.  $\mu_2$  and  $\mu_3$  are assumed to vary within a reasonable range in these figures. It can be seen from these figures that the optimum design parameters are proportional to  $\mu_2$  and non-proportional to  $\mu_3$ . Besides, it is obvious that the influence of  $\mu_2$  is more significant than that of  $\mu_3$  on the optimum design parameters. Most importantly, the analysis results indicate that higher  $\xi_2$ ,  $f_2$  and  $f_3$  may not be beneficial for the BMD design when  $\mu_3$  becomes larger.

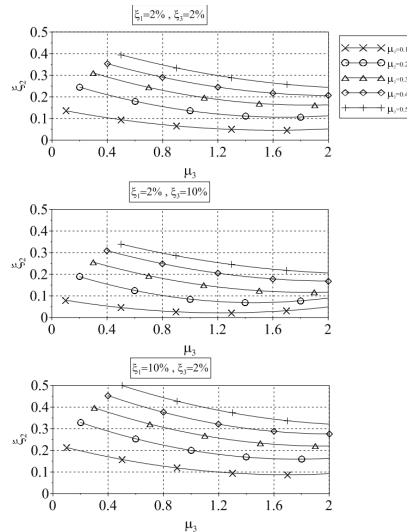


Figure 2.2  $\xi_2$  varying with respect to  $\mu_2$  and  $\mu_3$

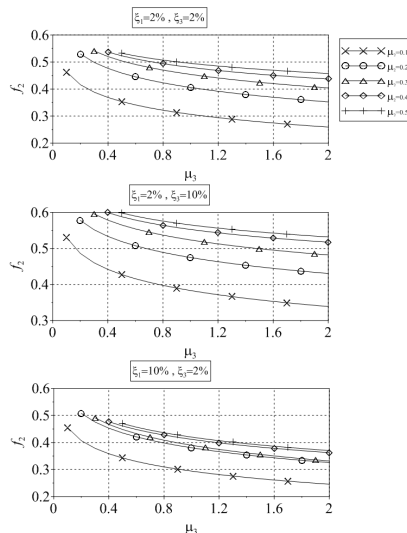


Figure 2.3  $f_2$  varying with respect to  $\mu_2$  and  $\mu_3$

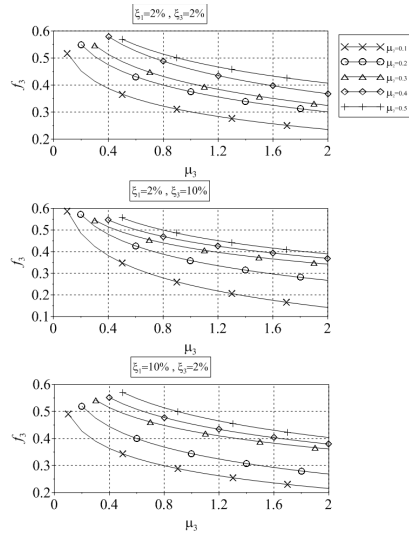


Figure 2.4  $f_3$  varying with respect to  $\mu_2$  and  $\mu_3$

### 3. EXPERIMENTAL STUDY

The effectiveness of the BMD system with optimum design parameters on the seismic protection of building structures is evaluated through a series of shaking table tests.

#### 3.1 Design of Test Specimen with BMD System

Considering a scale-down factor of 1/4, the plane dimension and height of each story of the test steel structures are 1500mm by 1100mm and 1100mm, respectively. The columns are wide flange sections with a sectional- dimension of 100×100×6×8 (mm), and the beams are channel sections with a sectional-dimension of 100×50×5×5 (mm). The material properties of the columns and beams are A36 steel. In this study, the total heights of two types of test specimens, Specimens A and B, are the same but the isolation systems are installed at two different stories (or two different elevations), as shown in Fig.5. Specimen A consists of 4-story superstructure, isolation system composed of rubber bearings (RB) and linear viscous dampers (VD), and 3-story substructure. Specimen B consists of 6-story superstructure, isolation system composed of RBs and linear VDs, and 1-story substructure. A seismic reactive mass of 0.5 kN-sec<sup>2</sup>/m is assigned to each floor of Specimens A and B.

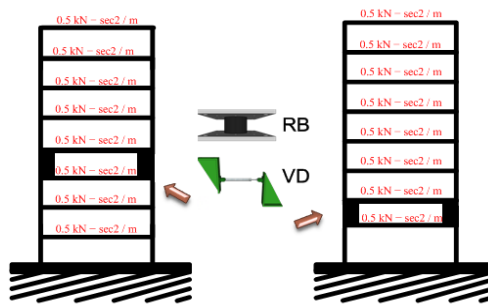


Figure 3.1 Design drawings of Specimens A and B

After calculating the predominant modal masses and modal periods of the substructure and superstructure with a fixed base condition for each test specimen, the author-defined parameters and the optimum design parameters  $\xi_2$ ,  $f_2$  and  $f_3$  can be determined using the proposed method described in Section 2.2. It is apparent that different mass ratio cases may result in different optimum design values of  $f_3$ . Therefore, for the optimum design purpose, the superstructure of Specimen B needs to be stiffened because the original value of  $f_3$  (i.e.  $f_{3,design}$ ) is smaller than the optimum value of  $f_3$  (i.e.

$f_{3,optimum}$ ), while the substructure of Specimen A needs to be stiffened due to a smaller demand for  $f_2$ . The angle-section steel braces with different section dimensions are designed and installed in the superstructure or substructure in order to achieve the design objectives. The stiffness contributed by RBs and the equivalent damping ratio of linear VDs in the isolation layer can be calculated according to the determined optimum values and  $f_2$  and  $\xi_2$ , respectively. The preliminary design procedure is illustrated in Fig. 3.2. The optimum design results for Specimens A and B, denoted as Specimens A-1 and B-1 thereafter and depicted in Fig. 3.3, are summarized in Table. 3.1.

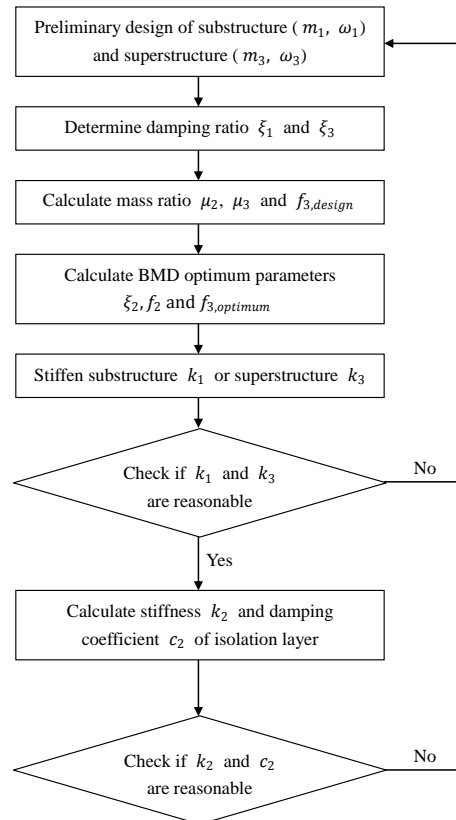


Figure 3.2 Design procedure of BMD system



Figure 3.3 Photos of Specimens A-1 and B-1 on shaking table

In order to verify the validity of the proposed method for optimum BMD design, as well as to discuss the influences of the parameters of interest on seismic control, a series of benchmark building structures are also designed and fabricated as described in the following:

- (1) Compared to Specimen A-1, Specimen A-2 has a lower stiffness contributed by RBs  $k_2$  (or nominal frequency  $\omega_2$ ) while Specimen A-3 has a higher one. Meanwhile, in order to fix the component damping ratio  $\xi_2$  which is related to  $\omega_2$ , the damping coefficients of linear VDs for Specimens A-2 and A-3 should also be adjusted adequately.
- (2) Specimen A-4 has a lower  $\xi_2$  while Specimen A-5 has a higher one, compared to Specimen A-1
- (3) Compared to Specimen A-1, Specimen A-6 has a lower substructure stiffness  $k_1$  (or nominal frequency  $\omega_1$ ) while Specimen A-7 has a higher one. Meanwhile, because the variation of  $\omega_1$  also leads to the variations of  $f_2$  and  $f_3$ , the damping coefficients of linear viscous dampers for Specimens A-6 and A7 should also be adjusted adequately.
- (4) Specimen B-2 has a lower superstructure stiffness  $k_3$  (or nominal frequency  $\omega_3$ ) while Specimen B-3 has a higher one, compared to Specimen B-1

The non-optimum design results for Specimens A and B, including Specimens A-2, A-3, A-4, A-5, A-6, A-7, B-2 and B-3, together with the design results for the bare frame structure, are summarized in Table. 1.

Table. 3.1. Design parameters for all test specimens

Specimen	Structural Parameter			Stiffness of RB kN/m	Damping of VD kN-s/m	Brace section (mm)
	$\xi_2$	$f_2$	$f_3$			
Bare Frame	-	-	-	-	-	-
A-1	0.22	0.43	0.47	952.57	25.56	L70×70×6
A-2	0.22	0.29	0.47	435.13	17.28	L70×70×6
A-3	0.22	0.53	0.47	1470	31.88	L70×70×6
A-4	0.09	0.43	0.47	952.57	10.46	L70×70×6
A-5	0.35	0.43	0.47	952.57	40.67	L70×70×6
A-6	0.22	0.43	0.52	811.93	23.6	L60×60×5
A-7	0.22	0.43	0.42	1226.3	29	L90×90×9
B-1	0.28	0.45	0.4	1452.29	46.98	L20×20×2
B-2	0.28	0.45	0.34	1452.29	46.98	L15×15×1
B-3	0.28	0.45	0.45	1452.29	46.98	L25×25×3

### 3.2 Input Ground Motion

Five real earthquake records with distinct seismic characteristics adopted in this research, including 1999 Taiwan Chi-Chi earthquake recorded at TCU047 and TCU068 stations, 1940 United States Imperial Valley earthquake recorded at I-ELC270 station, 1995 Japan Kobe earthquake recorded at KJM000 station, and 2011 off the Pacific coast of Tohoku earthquake recorded in the THU building close to MYG013 station (respectively denoted as TCU047, TCU068, EL Centro, Kobe and THU thereafter), are summarized in Table. 3.2. The critical component of each earthquake time history that possesses a larger peak ground acceleration (PGA) value is chosen for the ground input of the shaking table tests. Furthermore, since the test specimens are scale-down building structures, a time scale ( $= \sqrt{\text{scale factor}} = 1/\sqrt{4}$ ) should be considered for all the earthquake excitations to meet the similitude law. The scaled acceleration spectra for all the test earthquake excitations normalized to a PGA value of 1g are illustrated in Fig. 3.4.

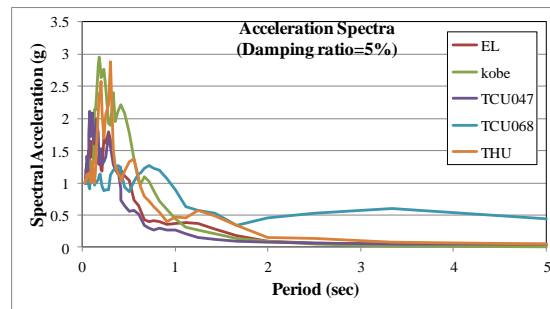


Figure 3.4 Acceleration spectra of earthquake excitations

Table. 3.2. Earthquake test program

Test Name	Input Excitation	Earthquake Component	Time Scale	Shaking Direction	Test PGA Original PGA	Test PGA Value (g)
I-ELC270	El Centro/I-ELC270 Imperial Valley, U.S. 1940/05/19 Real Earthquake	NS	$\sqrt{\text{scale factor}} = 1/\sqrt{4}$	X	80%	0.28g
					160%	0.56g
					240%	0.84g
KJM000	KJMA/KJM000 Kobe, Japan 1995/01/16 Real Earthquake	NS	$\sqrt{\text{scale factor}} = 1/\sqrt{4}$	X	40%	0.33g
					60%	0.50g
					80%	0.66g
921TCU047	Chi-Chi/TCU047 Chi-Chi, Taiwan 1999/09/21 Real Earthquake	NS	$\sqrt{\text{scale factor}} = 1/\sqrt{4}$	X	80%	0.35g
					160%	0.70g
					240%	1.06g
921TCU068	Chi-Chi/TCU068 Chi-Chi, Taiwan 1999/09/21 Real Earthquake	NS	$\sqrt{\text{scale factor}} = 1/\sqrt{4}$	X	30%	0.19g
					60%	0.37g
					90%	0.56g
THU	Tohoku/THU Tohoku, Japan 2011/03/11 Real Earthquake	NS	$\sqrt{\text{scale factor}} = 1/\sqrt{4}$	X	50%	0.17g
					100%	0.33g
					150%	0.50g

### 3.3 Seismic Response

The comparison of peak acceleration responses at each story of Specimen A-1 and the bare frame structure under EL Centro and TCU068 earthquakes is shown in Fig. 3.5. It can be seen that the structure with optimum BMD design can reveal a better seismic performance compared to the bare frame structure. That is to say, the BMD system with optimum design parameters is beneficial as expected for structural control.

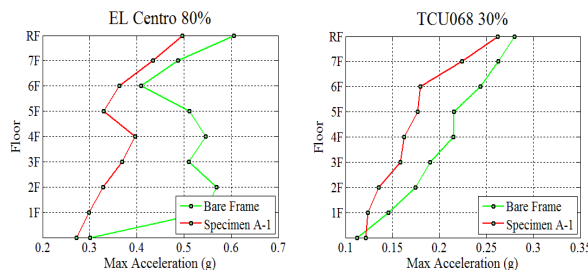


Figure 3.5 Peak acceleration responses of Specimen A-1 and bare frame structure

The peak acceleration responses at each story of Specimens A-1, A-2 and A-3 subjected to all the earthquake excitations are depicted in Fig. 3.6. The values of  $f_2$  for Specimens A-1, A-2 and A-3 are 0.43 (optimum design value), 0.29 and 0.53, respectively, as summarized in Table. 3.1. It is of no surprise that more flexible the isolation system is (i.e.  $f_2$  is smaller), smaller acceleration responses the superstructure has. On the contrary, a stiffer isolation system (i.e.  $f_2$  is larger) would lead to larger acceleration responses at both the superstructure and substructure. Besides, although there is no significant difference between the peak acceleration responses at the superstructures of Specimens A-1 and A-2, the flexibility of the isolation system may result in enlarged acceleration responses at the substructure. In summary, Specimen A-1 for which the optimum BMD design parameters are designed has a better seismic control capability than Specimens A-2 and A-3.

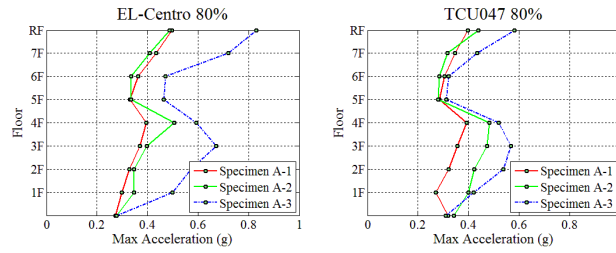


Figure 3.6 Peak acceleration responses of Specimens A-1, A-2 and A-3

The peak acceleration responses at each story of Specimens A-1, A-4, and A-5 under all the earthquake excitations are depicted in Fig. 3.7. The values of  $\xi_2$  for specimens A-1, A-4 and A-5 are 22% (optimum design value), 9% and 35%, respectively, as summarized in Table. 1. It is of no surprise that Specimen A-4 reveals a worse seismic performance compared to Specimens A-1 and A-5 due to a smaller  $\xi_2$  value (i.e.  $\xi_2=9\%$ ). It is worth noting that the reduction of acceleration response in Specimen A-1 with the optimum design value (i.e.  $\xi_2=22\%$ ) is similar to and even better than that in Specimen A-5 with a larger  $\xi_2$  (i.e.  $\xi_2=35\%$ ). In other words, an increase of  $\xi_2$  is not very beneficial for acceleration reduction when  $\xi_2$  is larger than the optimum design value, especially at the superstructure.

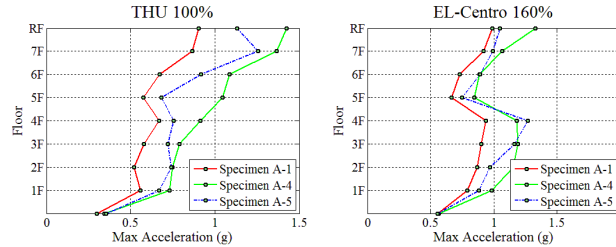


Figure 3.7 Peak acceleration responses of Specimens A-1, A-4 and A-5

The peak acceleration responses at each story of Specimens A-1, A-6, and A-7 under all the earthquake excitations are depicted in Fig. 3.8. The values of  $f_3$  for Specimens A-1, A-6 and A-7 are 0.47 (optimum design value), 0.52 and 0.42, respectively, as summarized in Table. 1. It can be seen that the influence of  $f_3$  on the acceleration responses at the substructure is more significant than that at the superstructure. It should be noted that the peak acceleration response at the substructure is increased significantly with increasing  $f_3$  under TCU047 and THU. The effect of  $f_3$  on the seismic performance of a building structure with the BMD system should be further studied after the test data are processed completely.

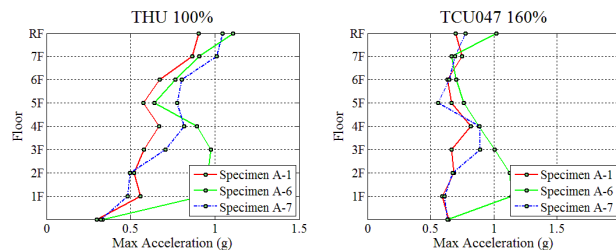


Figure 3.8 Peak acceleration responses of Specimens A-1, A-6 and A-7

Based on the preliminary experimental results, it can be concluded that Specimen A-1 for which the optimum BMD design parameters are designed has a satisfactory seismic performance.

#### 4. CONCLUSIONS

Using the simplified structural model and the proposed objective function, the effects of different parameters of interest, including mass ratios, frequency ratios and damping ratios, on the dynamic characteristics of a building structure with the BMD system are investigated thoroughly in this study. The preliminary experimental results indicate that the BMD system with optimum design parameters can effectively control the seismic responses of both the superstructure and substructure. Therefore, the complete experimental data will be further studied and the comparison of numerical predictions and experimental results will be performed in the next stage of this research. Based on the experimental and numerical results, it is the final goal to provide an appropriate and feasible design procedure for a building structure with the optimum BMD system in practice.

#### References:

- Koh T and Kobayashi M. Vibratory Characteristics and Earthquake Response of Mid-Story Isolated Buildings. *Memoirs of the Institute of Sciences and Technology, Meiji University*, 2000; 39(12): 97-114.
- Wang SJ, Chang KC, Hwang JS and Lee BH. Simplified Analysis of Mid-Story Seismically Isolated Buildings. *Earthquake Engineering and Structural Dynamics*, 2011; 40(2): 119-133.
- Asher, JW, Young, RP and Ewing RD, Seismic isolation of the arrowhead regional medical center, The structural design of tall buildings, Vol. 10, p. 321-334, 2001.
- Chang, K. C., Hwang, J. S., Chan, T. C., Tau, C. C. and Wang, S. J., "Application, R&D and Design Rules for Seismic Isolation and Energy Dissipation Systems for Buildings and Bridges in Taiwan," Proceedings of the 10th World Conference on Seismic Isolation, Energy Dissipation and Active Vibrations Control of Structures, Istanbul, Turkey, May 28-31, 2007.
- K. C. Chang, J. S. Hwang, S. J. Wang, B. H. Lee, J. Y. Hsiao and Y. C. Hung, "Shaking Table Tests of Scaled Buildings Isolated at Different Stories," Proceedings of the 11th World Conference on Seismic Isolation, Energy Dissipation and Active Vibration Control of Structures, Guangzhou, China, November 17-21, 2009.
- Den Hartog, J. P. (1956) . *Mechanical Vibrations*, 4th edition, McGraw-Hill, New York
- McNamara, R. J. (1977) . "Tuned Mass Dampers for Buildings", *Journal of the Structural Division, ASCE*, Vol. 103, pp. 1785-1798
- Luft, R. W. (1979) . "Optimal Tuned Mass Dampers for Buildings", *Journal of the Structural Division, ASCE*, Vol. 105, pp.2766-2772.
- Hsiang-Chuan Tsai and Guan-Cheng Lin (1993), "Optimum Tuned-Mass Dampers for Minimizing Steady-State Response of Support-Excited and Damped Systems," *Journal of Earthquake Engineering and Structural Dynamics*, Vol. 23, 957-973
- Sadek, F., Mohraz, B., Taylor, A. W., and Chung, R. M.. 'A method of estimating the parameters of tuned mass dampers for seismic applications'. *Earthquake Eng. struct. dyn.* 26(6), 617-637 (1997)
- Fujino, Y. and Abe, M. (1993) . "Design formulas for tuned mass dampers based on a perturbation technique", *Earthquake Engineering and Structural Dynamics*, Vol. 22, pp.833-854